Journal of Steroid Biochemistry and Molecular Biology 245 (2025) 106638

Contents lists available at ScienceDirect

Journal of Steroid Biochemistry and Molecular Biology

journal homepage: www.elsevier.com/locate/jsbmb

Effects of parabens on human and rat placental 3β-hydroxysteroid dehydrogenase isoforms: Structure activity relationship and docking analysis

Jie Xiang [a], Mingzhu Zhong [a], Qian Zhang [a], Yang Zhu [b], Peipei Pan [a], Huitao Li [b], Qianjin Fei [d,*], Rongying Ou [a,*], Ren-shan Ge [b,*], Weibing Zhang [c,*]

[a] Department of Obstetrics and Gynecology, the First Affiliated Hospital of Wenzhou Medical University, Wenzhou, Zhejiang 325027, China
[b] Department of Anaesthesiology, the Second Affiliated Hospital and Yuying Children's Hospital of Wenzhou Medical University, Wenzhou, Zhejiang 325027, China
[c] Department of Pharmacy, the First Affiliated Hospital of Wenzhou Medical University, Wenzhou 325015, China
[d] Reproductive Medicine Centre, the First Affiliated Hospital of Wenzhou Medical University, Wenzhou 325015, China

ARTICLE INFO

Keywords:
Parabens
Progesterone
Pregnenolone
3β-HSD
Placenta

ABSTRACT

Parabens are widely used as preservatives in personal care products and are linked to potential disruptions in placental steroidogenesis. However, their exact impact remains unclear. This study aimed to explore the inhibition, mechanisms, structure-activity relationships (SAR) of parabens on human placental 3β-hydroxysteroid dehydrogenase type 1 (h3β-HSD1) and its rat counterpart, r3β-HSD4.3β-HSD activity was assayed in placental microsomes using pregnenolone as substrate and HPLC-MS/MS to measure progesterone and the effects of parabens on 3β-HSD was evaluated and SAR was performed. The research identified their inhibition against h3β-HSD1, with nonylparaben showing the highest potency (IC_{50}, 4.17 μM), followed by phenylparaben, heptylparaben, hexylparaben, benzylparaben, butylparaben, propylparaben, and ethylparaben. The inhibition was characterized as mixed/noncompetitive. Additionally, these parabens inhibited progesterone secretion in human JAr cells at ≤100 μM. Similar trends were observed for r3β-HSD4. Docking simulations indicated that parabens interact with NAD^+ and steroid-binding sites of both enzymes. A negative correlation between LogP, molecular weight, volume, and alcohol chain carbon with IC_{50} values highlighted the role of carbon chain length in determining inhibitory efficacy. The inhibitory potency of parabens on 3β-HSD is significantly influenced by their structural attributes, particularly the length of their carbon chains and LogP values.

1. Introduction

Parabens (Fig. 1A), a group of alcohol esters derived from 4-hydroxybenzoic acid (also known as paraben acid), are extensively utilized in the preservation of packaged foods, pharmaceuticals, and cosmetics [1]. Variations in the alkyl or aromatic groups present in the alcohol moiety result in distinct types of parabens, such as methylparaben, ethylparaben, propylparaben, butylparaben, hexylparaben, heptylparaben, nonylparaben, benzylparaben, and phenylparaben [1]. Renowned for their antimicrobial properties that thwart bacterial and yeast growth in these products, parabens serve as effective preservatives in a wide array of personal care and cosmetic items and foods, as well as pharmaceuticals [2]. Despite being generally deemed safe for application, there has been a recent surge in controversy surrounding potential estrogenic effects of parabens and their purported links to contact dermatitis and breast cancer [3–6], likely attributed to their function as mild estrogens [3]. The existing scientific literature on the health implications of parabens remains inconclusive, albeit certain epidemiological studies have associated these compounds with endocrine disruptions [4,7–9].

Beyond their estrogenic activity, some parabens may interfere with steroidogenesis of steroid hormones. Previous studies have demonstrated the inhibitory effect of parabens on 17β-hydroxysteroid dehydrogenase type 1 (17β-HSD1), a member in the short-chain dehydrogenase/reductase (SDR) family and an enzyme crucial for the conversion of estrone to active estradiol [10]. Additionally, other steroidogenic enzymes could potentially be targeted by parabens. Among these enzymes is human 3β-hydroxysteroid dehydrogenase/Δ^5-Δ^4 isomerase (h3β-HSD1), another SDR member and a pivotal enzyme

* Corresponding authors.
E-mail addresses: feiqianjin@163.com (Q. Fei), ourongying@163.com (R. Ou), renshan_ge@wmu.edu.cn (R.-s. Ge), 122657737@qq.com (W. Zhang).

https://doi.org/10.1016/j.jsbmb.2024.106638
Received 23 September 2024; Received in revised form 13 November 2024; Accepted 14 November 2024
Available online 19 November 2024

involved in the biosynthesis of most steroid hormones [11,12]. Specifically, h3β-HSD1 plays a critical role in the conversion of pregnenolone (P5) to progesterone (P4) in various tissues (Fig. 1B), including the placenta, with its enzymatic activity requiring a cofactor, NAD^+. The h3β-HSD1 belongs to the SDR family and has clear catalytic residues, including Ser124, Tyr155, and Lys159 [12].

In exploring the mechanisms underlying the inhibition of h3β-HSD1 by parabens, understanding the impact of various substituents in the alcohol moiety on their structure-activity relationship (SAR) and mode of action is crucial. Utilizing three-dimensional quantitative SAR (3D-QSAR) analysis can shed light on the intricate interactions between different parabens and the target enzyme h3β-HSD1 within the human body.

Moreover, conducting comparative analyses of paraben effects on placental 3β-HSD enzymes across different species, such as humans and rats, particularly focusing on rat placental homolog 3β-HSD4 (r3β-HSD4) is prevalent [12], offers valuable insights into potential species-specific variations in their physiological effects and influence on steroidogenesis pathways. The goal of this study is to identify the hazards associated with paraben compounds. These comparative investigations play a pivotal role in evaluating the translational relevance of findings obtained from animal studies to human contexts, thereby informing more accurate risk assessment protocols concerning paraben exposure.

2. Materials and methods

2.1. Materials and animals

P5 and progesterone were obtained from Steraloids (Newport, RI, USA). Methylparaben (CAS: 99–76–3, Cat.: M108621, purity >98 %) was acquired from Aladdin (Shanghai, China), ethylparaben (CAS: 120–47–8, Cat.: E808808, purity >99 %), propylparaben (CAS: 94–13–3, Cat.: P815728, purity >99 %), butylparaben (CAS: 94–26–8, Cat.: B802592, purity >98 %), hexylparaben (CAS: 1083–27–8, Cat.: H862720, purity >98 %), heptylparaben (CAS: 1085–12–7, Cat.: H859347, purity >98 %), nonylparaben (CAS: 38713–56–3, Cat.: N863034, purity >98 %), and benzylparaben (CAS: 94–18–8, Cat.: 802025, purity >98 %) from Maclin (Shanghai, China), phenylparaben (CAS: 17696–62–7, Cat.: H0218, purity >98 %) from TCI chemical (Shanghai, China), as well as sucrose, dimethyl sulfoxide (DMSO, analytical grade), phosphate-buffered saline (PBS, pH 7.2), and NAD^+

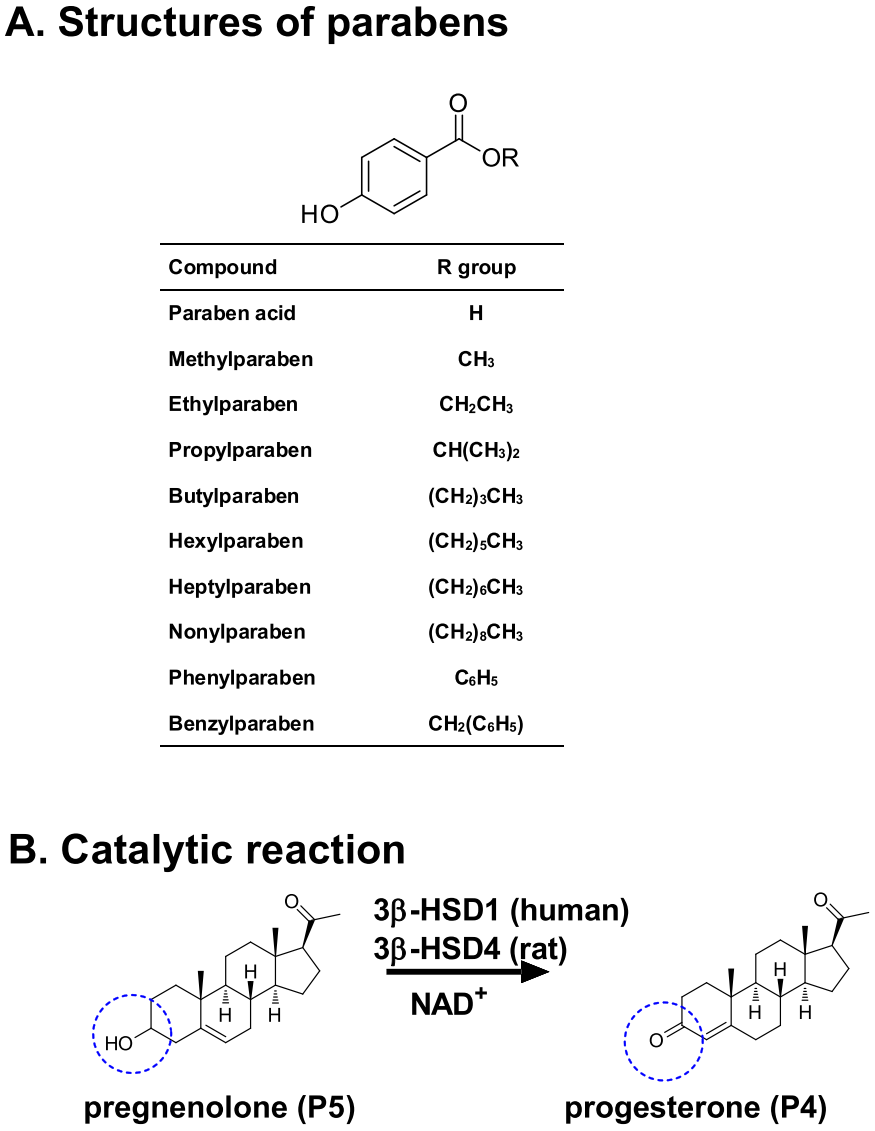

Fig. 1. Chemical Structures and Enzymatic Reaction of Parabens and 3β-Hydroxysteroid Dehydrogenase (3β-HSD) (A) Structures of Parabens: This panel illustrates the chemical structures of various parabens, highlighting their common ester functional groups; (B) 3β-HSD Reaction: This section details the enzymatic process where 3β-HSD catalyses the conversion of pregnenolone (P5) into progesterone (P4), a critical step in steroidogenesis.

from Sigma-Aldrich (Louis, MO, USA). Pregnant (15 days of conception) Sprague-Dawley rats were sourced from the Shanghai Laboratory Animal Center (Shanghai, China) and dams were euthanized by CO_2 at pregnancy of 20 days for collection of placentas, which was subsequently stored at −80°C. The use of animals in this study was ethically sanctioned by the Experimental Animal Ethics Committee of Wenzhou Medical University, adhering to the guidelines in the Guide for the Care and Use of Experimental Animals (NIH). Human placentas (full-term) were obtained from the Second Affiliated Hospital of Wenzhou Medical University, with the research approved protocol (number 2022-K-81–01) issued by the Clinical Research Committee of Wenzhou Medical University Second Affiliated Hospital, ensuring compliance with all ethical and procedural standards and consent by the patients.

2.2. JAr cell culture and progesterone production experiments

Human choriocarcinoma JAr cells (ATCC, USA) were cultured as previously described [13]. Specifically, the human JAr cells were propagated in RPMI-1640 medium enriched with 10 % heat-inactivated steroid-free fetal calf serum (Invitrogen, USA) and incubated at 37°C within a humidified environment containing 5 % CO_2. For experimental purposes, these cells were seeded at a density of 10^6 cells per well in the 24-well plate containing 1 mL of medium and subsequently exposed to varying concentrations of parabens (1, 10, 20, 50, and 100 μM) alongside a control group (DMSO) for 24 hrs. After treatment, the media were collected and 100 μL of medium was adopted for the quantification of P4 levels as follows using HPLC-MS/MS.

2.3. Preparation of microsomes

Microsomes were prepared from human and rat placentas as previously described [14]. In brief, a piece of placental tissue was homogenized in a buffer consisting of 0.01 M PBS (pH 7.2) supplemented with 0.25 M sucrose using a glass homogenizer. This homogenate was then subjected to centrifugation steps: 700 × g for 30 min to remove large debris and nucleus, 14,500 × g for 30 min to remove mitochondria, and finally, 105,000 × g for 60 min twice to obtain microsomal pellet fraction. The microsomal pellets were resuspended using a glass homogenizer. The protein concentrations of microsomal fractions were quantified using a BCA protein assay kit (Cat. P0010, Beyotime, Shanghai, China) using plate reader as previously described [14].

2.4. Detection of 3β-HSD activity in microsomal suspension

The enzymatic activity of h3β-HSD1 or r3β-HSD4 within microsomal suspensions was assessed as previously described [15]. Specifically, the assay involved the incubation of a 100 μL PBS solution (0.01 M, pH 7.2) containing fixed concentration or a range of concentrations of P5, 0.2 mM NAD^+, and 1 μg of microsomal protein in a 1.5 mL test tube and the mixture was incubated at 37°C in a shaking water bath (75 rpm) at 60 min to facilitate the 3β-HSD reaction for the conversion of P5 to P4 in a linear reaction range. A series of experiments were conducted: 1) Michaelis constant (Km) determination: a range of P5 (0, 0.1, 0.3, 0.5, and 1 μM) was tested in the basic reaction condition. 2) Screening assay: parabens (final concentration of 100 μM) dissolved in DMSO and 200 nM P5 were incubated in the basic reaction condition. 3) IC_{50} (half-maximum inhibitory concentration) determine: a range of concentrations of parabens (0, 0.1, 1, 5, 10, 50, 100, and 200 μM) and 200 nM P5 were incubated in the basic condition. 4) Mechanism determination: a range of concentrations of parabens (0–100 μM) and a range of concentrations of P5 were incubated in the basic conditions. Upon completion of the reaction, in the tube, 10 μL of an internal reference substance (Testosterone-d5, Shanghai Zzbio Co., China) and 200 μL of acetonitrile (Merck Supelco, PA, USA) were added and the tube underwent mixing. The tube was centrifuged at 12,000 rpm for 10 min to separate the acetonitrile layer, which contained P5 and P4. Subsequently, 100 μL of acetonitrile was transferred to a sample bottle and 1 μL was automatically injected into HPLC-MS/MS for separation P5 and P4 and quantitation of P4.

2.5. HPLC-MS/MS condition for P4 quantification

P4 measurement was achieved utilizing an Acquity HPLC/MS−MS system (Waters, USA), configured with an Acquity BEH C18 column (2.1 mm × 50 mm, 1.7 μm particle size) and a 0.2 μm stainless steel block filter, following a previously established protocol [16]. The analytical conditions were as follows: a flow rate of 0.40 mL/min, an injection volume of 10 μL, a column temperature of 30°C, and a sample temperature of 4°C. The identification of P4 and the reference compound was performed under a XEVO TQD triple quadrupole mass spectrometer equipped with an electrospray ionization source with Multiple Reaction Monitoring mode. The specific transitions monitored were m/z 315.16→96.92 for P4 and m/z 289.07→96.92 for T-d5. The concentration of P4 in the samples was determined through a standard curve method, ensuring accuracy and reproducibility in the quantification process.

2.6. Calculation of enzyme activity and inhibition parameters

The GraphPad software version 9.5 (GraphPad Inc, USA) was employed for comprehensive data analysis. Initially, a nonlinear regression analysis was performed using the Michaelis-Menten equation $V = \mathrm{VmaxApp}\frac{S}{\mathrm{KmApp}+S}$, where V signifies enzyme velocity (pmol/mg/min), VmaxApp denotes the apparent maximum enzyme velocity (pmol/mg/min), S represents the concentration of substrate P5, and KmApp signifies the apparent Michaelis constant (μM). Following this, a screening assay was implemented to evaluate the inhibition effects of parabens on 3β-HSD. The control group, treated with 1 % DMSO, was established as the baseline for residual activity (RA) at 100 %. Subsequently, the RA under the influence of 100 μM paraben was compared relative to the control. Furthermore, the determination of the IC_{50} value was executed through the application of a predefined equation: $\mathrm{RA}\ (\%) = \mathrm{bottom} + \frac{\mathrm{top-bottom}}{1+10^{(\mathrm{LogX}-\mathrm{LogIC}50)}}$, where RA (%) represents residual activity under various concentrations of the inhibitor, top and bottom denote the upper and lower limits of RA, respectively, with bottom being set to approach a "zero" value, and Hill slope is −1. For the analysis of enzyme kinetics-inhibition (mixed model), a series of equations were utilized for nonlinear regression, including $\mathrm{VmaxApp} = \frac{\mathrm{Vmax}}{1+\frac{[i]}{\alpha\times \mathrm{Ki}}}$, $\mathrm{KmApp} = \mathrm{Km}\frac{1+\frac{[i]}{\alpha\times \mathrm{Ki}}}{1}$, and $\mathrm{RA} = \mathrm{VmaxApp}\frac{S}{\mathrm{KmApp}+S}$, where Ki signifies the inhibition constant, [i] represents inhibitor's concentration, and α is a determinator of mode of action. The α value obtained from these analyses was instrumental in classifying the mode of action: in this model, an α value of 1 indicated noncompetitive inhibition; α values greater than 1 or less than 1 suggested mixed inhibition; a very low α value, nearly zero but not equal to zero, indicated uncompetitive inhibition; and a very high α value suggested competitive inhibition. Additionally, a Dixon plot was constructed to visualize the relationship between the inverse of velocity (1/V) and the inhibitor's concentration ([i]), providing a linear representation of the data.

2.7. Molecular docking analysis of parabens with 3β-HSD

Due to the unavailability of crystal structures for h3β-HSD1 and r3β-HSD4, 3D structures generated by Swiss Homology Model Server were utilized as docking targets as described [15]. Specifically, the h3β-HSD1 structure (P14060) and r3β-HSD4 structure (Q62878) were retrieved. These structures served as the basis for subsequent molecular docking studies. The optimization of the h3β-HSD1 and r3β-HSD4 protein structure was conducted as outlined in prior studies [17,18]. The anticipated 3D structure was validated using Discovery Studio Client

through the generation of a Ramachandran plot [18]. The validity of the 3D structures was confirmed to the previously reported value [15]. The chemical and structural parameters of parabens, the compounds under investigation, were sourced from PubChem. Molecular docking simulations were executed using AutoDock 4.0, as previously detailed [19], to determine the lowest binding energy (ΔG, in kcal/mol), which can divide various energies including van der Waals, hydrogen bond (HB), desolvation energy, etc. The 3D structures were prepared using PyMOL, and 2D representations of overlapping residues between the chemicals and the substrate were generated using Discovery Studio, along with an illustration of hydrogen bonds (HBs). Furthermore, hydrophobic interactions, π-stacking, and HBs were analysed through the Discovery Studio, providing a comprehensive view of the molecular interactions involved. This approach not only facilitated the understanding of the binding mechanisms but also highlighted the potential of structures in advancing our knowledge of enzyme-substrate interactions.

2.8. Pearson correlation analysis

In the pursuit of elucidating the correlation between the IC_{50} values of parabens and diverse structural attributes, including LogP, molecular weight, heavy atoms, carbon number in the alcohol portion, data was extracted from the ZINC 2.0 database [20] as well as ΔG (interaction with the enzyme) from Autodock 4.0. We also retrieved the solubility, including LogS (the logarithm of the aqueous solubility), and permeability, including Caco-2 (a human colon adenocarcinoma cell line) and MDCK (Madin-Darby Canine Kidney cell) permeability for parabens from ADMETlab 2.0 as described [21]. These aforementioned parameters were systematically paired for parabens to facilitate analysis. Furthermore, an array of additional structural characteristics, such as hetero atoms, ring number, fraction sp3, net charge, hydrogen bond donor, hydrogen bond acceptor, tPSA, and rotation bonds, were subjected to a thorough visual inspection. This examination revealed that these features bore no discernible direct correlation with the IC_{50} values. To quantitatively evaluate the strength and direction of the relationship between the selected structural parameters and IC_{50} values, Pearson's correlation coefficient was employed.

2.9. 3D-QSAR analysis

In the process of generating and validating 3D-QSAR pharmacophores for parabens targeting human h3β-HSD1, a comprehensive analysis was conducted using the Discovery Studio Client software. A curated set of ligands, which included resveratrol derivatives (pinostilbene, pinosylvin, lunularin) [22], bisphenol A derivatives (bisphenol G, diallyl BPA) [23], saturated fatty acid compound (lauric acid) [24], benzene derivatives (phenylhexane) [24], flavone (apigenin) [25], pentahydroxyflavone (quercetin) [25], as well as parabens (heptylparaben, benzylparaben, butylparaben, in this study), was assembled as training dataset. These ligands, characterized by a broad spectrum of chemical structures and activities, were selected based on their IC_{50} values, which denote their potency in inhibiting h3β-HSD1. The optimization of these ligands was achieved through a refinement of their geometry and energy using a molecular mechanic force field. To facilitate the subsequent pharmacophore modelling, the ligand dataset was meticulously aligned in a common reference frame. This alignment was guided either by the structural similarity among the ligands or by the specific contours of the active site of the target protein. Following this alignment, a pharmacophore hypothesis was formulated to pinpoint the common features that are instrumental in the inhibition of h3β-HSD1. These features included hydrophobic regions (HY) and hydrogen bond donors (HBD), which are critical for the interaction with the target enzyme. Ten pharmacophore models were then generated, each reflecting the optimal positions and orientations of these features relative to the aligned ligands. To ascertain the predictive efficacy of these pharmacophore models in evaluating the activities of novel ligands, a stringent validation process was implemented using test dataset including ethylparaben, nonylparaben, phenylparaben, hexylparaben, propylparaben and other known chemicals (resveratrol [22], bisphenol AP and bisphenol B [23]). This validation involved the calculation of a "Fit value," which is derived from the sum over mapped features of weight(f) ×[1 - SSE(f)], where SSE(f) represents the sum over location constraints c on feature f of (D (c) / T (c))2. Here, D signifies the displacement of the feature from the centre of the location constraint, and T denotes the radius of the location constraint sphere for the feature, which defines the tolerance. A higher Fit value is indicative of a superior level of fitting, thereby validating the pharmacophore model's utility in predicting the inhibitory activities of new ligands against h3β-HSD1.

2.10. Statistics

The test was repeated four−eight times. The enzyme results were analysed by one-way analysis of variance (ANOVA) followed by post hoc Turkey's multiple comparisons to compare the significant difference. The significant differences were expressed as ^{a} $P < 0.05$, ^{b} $P < 0.01$, and ^{c} $P < 0.001$. The data are expressed as mean ± SEM (standard error of mean).

3. Results

3.1. Effect of parabens on h3β-HSD1 and r3β-HSD4 activity

In the placenta, h3β-HSD1 and r3β-HSD4 play a crucial role in the conversion of P5 to P4 (Fig. 1B). The kinetic parameters of h3β-HSD1 enzyme were assessed, revealing a KmApp of 0.15 ± 0.06 μM (Fig. 2A), aligning with previously reported ranges [12]. The VmaxApp was determined to be 22.08 ± 2.99pmol/mg/min (Fig. 2A). To investigate the effects of parabens on h3β-HSD1 activity, a screening for 10 compounds including 9 parabens and paraben acid was conducted at 100 μM. The results demonstrated that, with the exception of paraben acid and methylparaben, all other parabens significantly inhibited the h3β-HSD1 activity (Fig. 2B). Then, the kinetic parameters of r3β-HSD4 were also assessed, revealing a KmApp of 0.17 ± 0.05 μM (Fig. 2C), aligning with previously reported ranges [12]. The VmaxApp was determined to be 23.24 ± 3.28pmol/mg/min (Fig. 2C). To investigate the effects of parabens on r3β-HSD4 activity, a screening for these 10 chemicals was conducted at 100 μM. The results demonstrated that, with the exception of paraben acid and methylparaben, all other parabens significantly inhibited the r3β-HSD4 activity (Fig. 2D). These results suggest that some parabens can inhibit both h3β-HSD1 and r3β-HSD4 activity.

3.2. Inhibitory strength of parabens on h3β-HSD1 and r3β-HSD4 activity

Firstly, dose-response assays of parabens on h3β-HSD1, which exhibited less than 50 % residual activity compared to the control, yielded IC_{50} values ranged from 4.17 to 47.37 μM for nonylparaben to ethylparaben, respectively (Table 1). Further analysis through Ki determination confirmed these inhibitory effects, with Ki values on h3β-HSD1 ranged from 3.73 to 45.07 μM for nonylparaben to ethylparaben, respectively (Table 1). Secondly, dose-response assays of parabens on r3β-HSD4, which exhibited less than 50 % residual activity compared to the control, yielded IC_{50} values ranged from 14.92 to 146.54 μM for nonylparaben to ethylparaben, respectively (Table 1). Further analysis through Ki determination confirmed these inhibitory effects, with Ki values ranged from 14.34 to over 100 μM for nonylparaben to ethylparaben, respectively (Table 1). These data suggest a potency ranking of parabens as nonylparaben > phenylparaben > heptylparaben > hexylparaben > benzylparaben > butylparaben > propylparaben > ethylparaben > methylparaben. These results also indicate that r3β-HSD4 is less sensitive to parabens than h3β-HSD1.

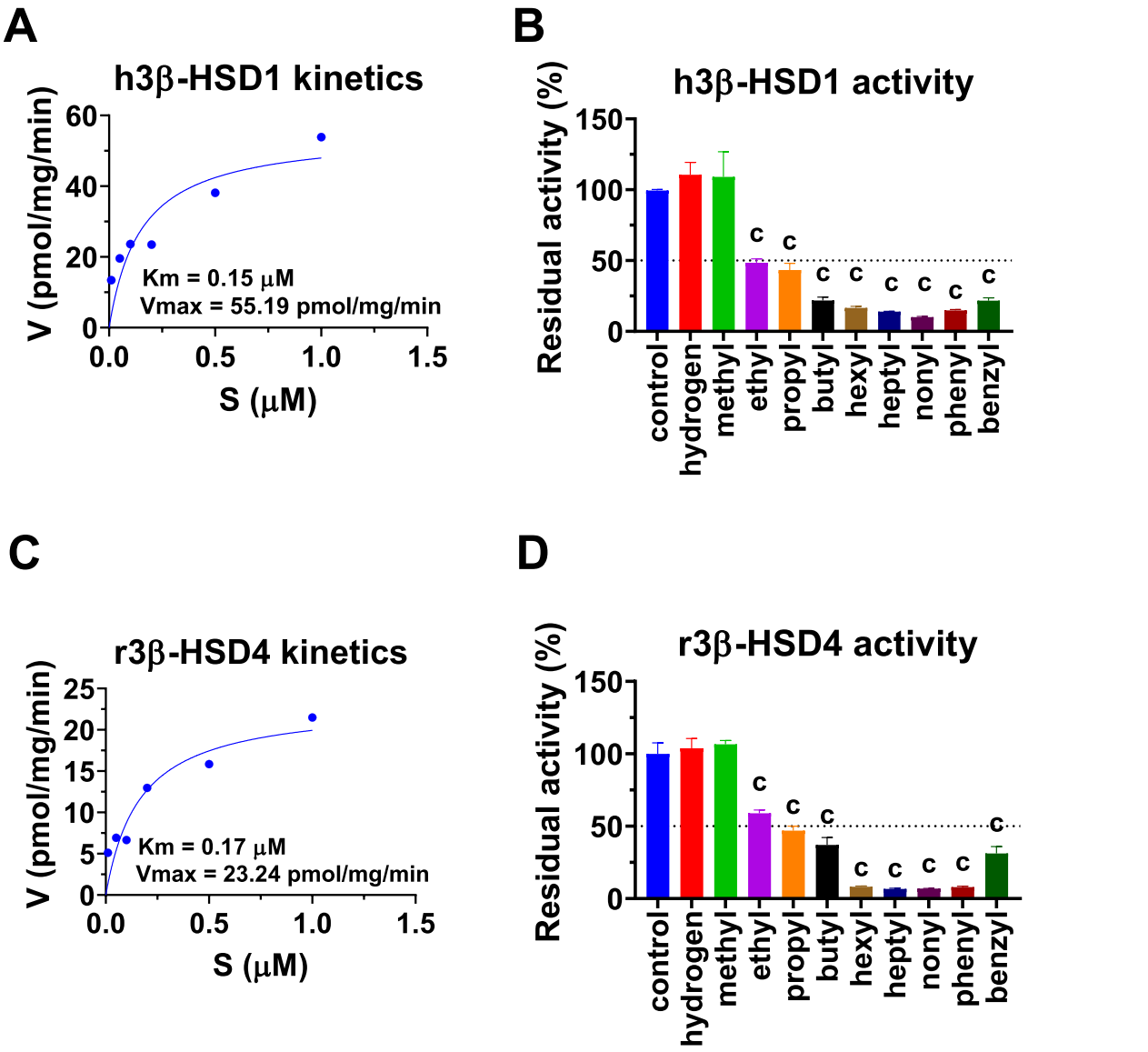

Fig. 2. Michaelis-Menten Kinetics and Inhibition Screening of Parabens on Human and Rat 3β-HSD (A) and (C) Michaelis-Menten Kinetics: These graphs depict the kinetic behaviour of human 3β-HSD1 (h3β-HSD1) and rat 3β-HSD4 (r3β-HSD4) in the presence of parabens, illustrating the relationship between substrate concentration and enzyme activity; (B) and (D) Residual Activity Relative to Control: These panels compare the residual enzyme activity in the presence of 100 μM parabens to a control (DMSO). Statistical significance is noted with $^{c}P<0.001$, based on n=4 replicates, each presented as mean ± SEM.

3.3. Inhibitory mode of parabens on h3β-HSD1 and r3β-HSD4

Examination of enzyme kinetics inhibition and Dixon plot analyses were conducted to elucidate the mechanism of action for both h3β-HSD1 and r3β-HSD4. Through these analyses, it was determined that all parabens exhibit a mixed or noncompetitive inhibition profile against these enzymes (Table 1, Fig. 3&Fig. S1 for h3β-HSD1, as well as in Fig. 4&Fig. S2 for r3β-HSD4). This classification of parabens as mixed or noncompetitive inhibitors indicates that these compounds interact with both the free enzyme and the enzyme-substrate complex of 3β-HSD to varying extents.

3.4. Inhibitory strength of parabens on P4 output in JAr cells

To investigate the potential of parabens to permeate cellular membranes and subsequently interfere with P4 secretion, human JAr cells were subjected to various concentrations of parabens for 24 hrs. As shown in Fig. 5, the study revealed that propylparaben, butylparaben, and benzylparaben exhibited a significant suppression of P4 production at various concentrations. Ethylparaben demonstrated a notable inhibition of P4 output at 10 μM and 100 μM. In contrast, hexylparaben, heptylparaben, and phenylparaben only significantly affected P4 secretion at the higher concentration of 100 μM. To our surprise, nonylparaben did not influence P4 levels across all tested concentrations nonylparaben despite exhibiting the highest inhibitory potency on h3β-HSD1. These findings underscore the importance of the penetration capability of parabens in their ability to exert hormonal effects, suggesting a complex interplay between chemical structure and cellular response. Indeed, through computer analysis by ADMETlab 2.0 analysis showed that the decreased solubility (LogS) and permeability (Caco-2 and MDCK cells, Table S1).

3.5. Molecular simulation analysis of parabens with h3β-HSD1 and r3β-HSD4

To elucidate the mode of action of parabens in relation to h3β-HSD1, we employed Autodock4 for molecular simulation analysis. The docking of P5 with h3β-HSD1 demonstrated that the 3β-hydroxyl group of P5

Table 1
Compound name, half-maximal inhibitory concentration (IC_{50}), inhibition constant (Ki), calculated Ki (Cal. Ki), lowest binding energy (ΔG), alpha, mode of action, and binding sites of parabens.

Compound name	IC_{50} μM	Ki μM	Cal. Ki μM	ΔG kcal/mol	Alpha	Mode of action	Binding sites
	Human 3β-HSD1						
Ethylparaben	47.37±0.87	45.07±21.92	53.98	−5.82	2.66	Mixed	P5, NAD^+
Propylparaben	29.49±0.37	35.02±14.95	31.28	−6.15	13.70	Mixed	P5, NAD^+
Butylparaben	24.09±0.86	25.29±21.25	25.33	−6.27	0.57	Mixed	P5, NAD^+
Hexylparaben	10.65±0.31	9.58±9.35	11.54	−6.74	2.55	Mixed	P5, NAD^+
Heptylparaben	6.88±0.19	7.87±3.65	8.97	−6.89	2.89	Mixed	P5, NAD^+
Nonylparaben	4.17±0.12	4.39±3.11	6.34	−7.09	0.83	Noncompetitive	NAD^+
Phenylparaben	6.76±0.21	7.48±9.24	7.13	−7.02	0.41	Mixed	P5, NAD^+
Benzylparaben	16.97±0.87	16.41±14.06	15.93	−6.55	6.11	Mixed	P5, NAD^+
	Rat 3β-HSD4						
Ethylparaben	146.54±4.62	ND	ND	ND	ND	ND	ND
Propylparaben	110.05±2.38	98.45±72.73	118.9	−5.29	0.76	Mixed	P5, NAD^+
Butylparaben	72.27±1.78	70.53±48.82	82.27	−5.57	1.87	Mixed	P5, NAD^+
Hexylparaben	32.22±0.85	30.81±16.40	36.36	−6.06	1.63	Mixed	P5, NAD^+
Heptylparaben	23.15±0.63	28.74±20.85	27.54	−6.22	0.49	Mixed	P5, NAD^+
Nonylparaben	14.92±0.43	14.34±12.56	20.36	−6.40	0.87	Noncompetitive	NAD^+
Phenylparaben	25.98±0.70	32.07±20.04	36.30	−6.06	1.08	Noncompetitive	NAD^+
Benzylparaben	18.32±0.51	20.61±30.94	20.33	−6.4	0.43	Mixed	P5, NAD^+

Note: 3β-HSD1=3β-hydroxysteroid dehydrogenase 1; 3β-HSD4=3β-hydroxysteroid dehydrogenase 4; ND=no determination; P5=pregnenolone.

interacts directly with the catalytic residues Ser125 and Tyr155, thereby corroborating previously established models. Similarly, when P5 was docked with r3β-HSD4, the 3β-hydroxyl group was found to be in contact with the catalytic residues Thr125 and Tyr155, further substantiating the reported model. Initially, we conducted a docking simulation of nonylparaben, known to be the most potent inhibitor, with h3β-HSD1. The results showed that nonylparaben specifically binds to the NAD^+ binding site (Fig. 6A), suggesting its role as a noncompetitive inhibitor. Nonylparaben establishes two HBs: one between the 4-hydroxyl group of the nonylparaben and Ser124, and another between the keto group of the ether and Ile190 (Fig. 6B). Additionally, it exhibited van der Waals interactions with nine residues and hydrophobic interactions with six residues (Fig. 6B). The calculated ΔG value for nonylparaben binding to h3β-HSD1 was −7.09 kcal/mol, with a predicted Ki value of 6.34 μM, aligning well with the experimentally determined Ki value. Subsequently, nonylparaben was also docked with r3β-HSD4, revealing its binding to the NAD^+ binding site (Fig. 6C), thus confirming its noncompetitive inhibitor status. In this interaction, nonylparaben forms two HBs: one with Ala84 and the other with Leu15 (Fig. 6D). It also engaged in van der Waals interactions with 15 residues and hydrophobic interactions with a single residue (Fig. 6D). The ΔG value for this interaction was determined to be −6.40 kcal/mol, with a predicted Ki value of 20.36 μM. Further analysis involving other parabens docked with h3β-HSD1 showed that these compounds bind either to the NAD^+ binding site or to a region proximal to it (Fig. S3A), indicating a mixed noncompetitive inhibition mechanism. Detailed interactions of these parabens with h3β-HSD1 are graphically represented in Fig. S3, providing a comprehensive overview of their binding characteristics and potential impact on enzyme function. Final analysis involving other parabens docked with r3β-HSD4 showed that these compounds bind either to the NAD^+ binding site or to a region proximal to it (Fig. S4A), indicating a mixed or noncompetitive inhibition mechanism. Detailed interactions of these parabens with r3β-HSD4 are graphically represented in Fig. S4, providing a comprehensive overview of their binding characteristics and potential impact on enzyme function. The contributions of various energies were listed in Table S2.

3.6. SAR analysis for parabens with h3β-HSD1 activity

In our study, we delved into the structural determinants of parabens that correlated with the inhibitory IC_{50} values observed for h3β-HSD1 and r3β-HSD4. We examined various molecular characteristics of parabens, including LogP, molecular weight, and volume, carbon number of the alcohol moiety to elucidate their impact on the inhibitory potency against both enzymes. Our findings showed that the inhibitory efficacy of parabens on both enzymes was indeed influenced by these molecular attributes. Notably, we observed a significant inverse correlation between LogP, molecular weight, volume, carbon number and ΔG values of the alcohol moiety and IC_{50} values (Fig. 7); higher these structural values corresponded to lower IC_{50} values, indicating a more potent inhibition. This comprehensive analysis underscores the critical role of these molecular properties in modulating the biological activity of parabens.

3.7. 3D-QSAR analysis for parabens with h3β-HSD1 activity

We have developed 3D-QSAR pharmacophore models from various class of compounds that provide profound insights into the requisite structural elements for potent inhibitors of the h3β-HSD1 enzyme. Our analytical approach centred on three pivotal features: HBA, HBD, and HY. Among the various models generated, Hypo1 was identified as the preeminent hypothesis structure, substantiated by its superior performance metrics: a high correlation coefficient of 0.90, a RMSD of 0.84, and the lowest overall cost of 80.27 (Table S3). To rigorously evaluate the statistical robustness of the Hypo1 model, we employed the Fischer randomization test utilizing the CatScramble methodology. This procedure entailed the random reallocation of IC_{50} values among the compounds in the training set to construct hypothetical pharmacophores. The resultant correlation coefficient for the training set was 0.90, affirming the statistical validity of the model (Fig. 8 A and Table S4). The spatial arrangement of chemical features within the Hypo1 model spanned distances from approximately 4.77 to 13.06 Å (Fig. 8B). Application of the Hypo1 model to the most active compound, nonylparaben from test dataset (IC_{50} = 4.17 μM, Table S4), which contacted all HBA, HBD, and HY (Fig. 8 C), yielded a fitting value of 2.68, whereas the least active compound, ethylparaben from test dataset (IC_{50} = 47.37 μM, Table S4), which contacted only HBA and HBD without contacting with HY, demonstrated a diminished fit value of 1.78 (Fig. 8D). These findings underscore the efficacy of the Hypo1 model in discerning the inhibitory potential of parabens against h3β-HSD1, thereby enhancing our understanding of enzyme-inhibitor interactions and potentially guiding the identification of more effective (toxic) agents.

4. Discussion

The study investigated the inhibitory effects of various parabens on human and rat placental 3β-HSDs. The results demonstrated that

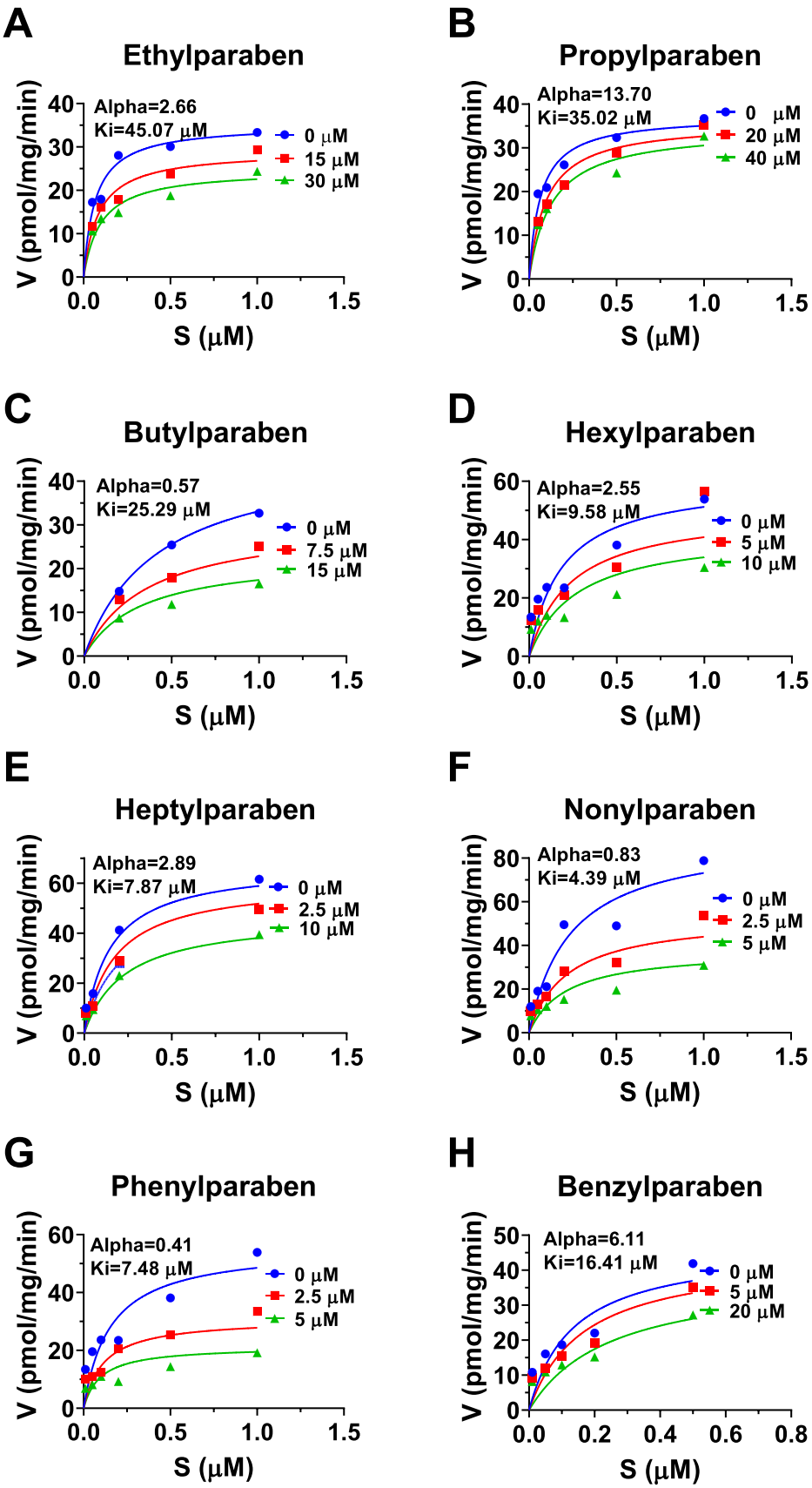

Fig. 3. Michaelis-Menten Kinetics Analysis (Mixed Model) of Parabens Inhibition on Human 3β-HSD1 (h3β-HSD1)This figure presents Michaelis-Menten Kinetics analysing the inhibition of h3β-HSD1 by eight different parabens (A-H). Incubation conditions included a temperature of 37°C, with pregnenolone (0.2 mM), NAD^+ (0.2 mM), human placental microsomes (10 μg), and varying concentrations of each paraben in 0.01 M PBS (pH 7.2). These plots provide a detailed view of the inhibition patterns and the impact of different paraben concentrations on enzyme activity.

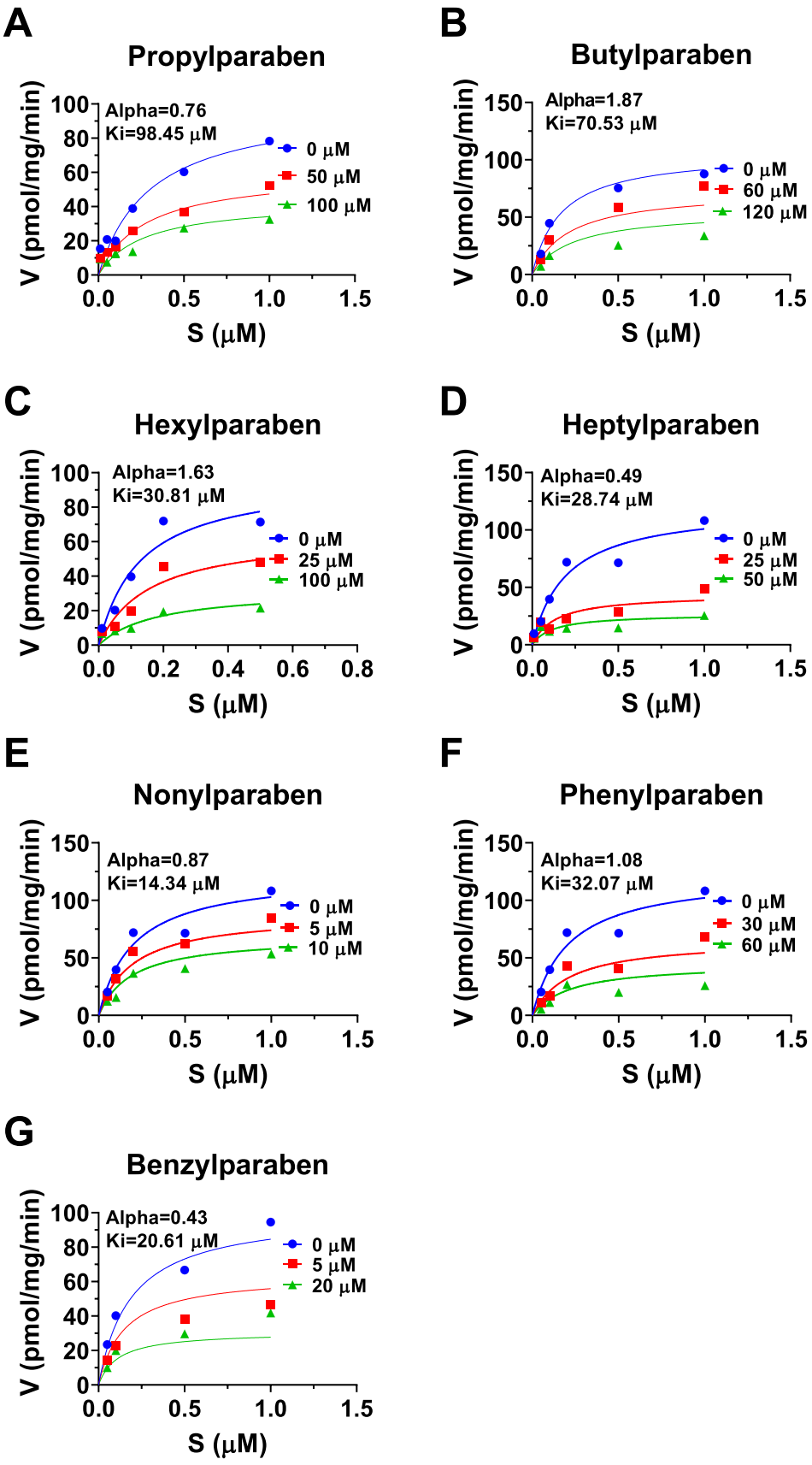

Fig. 4. Michaelis-Menten Kinetics Analysis (Mixed Model) on Rat 3β-HSD1 (r3β-HSD4)This figure presents Michaelis-Menten Kinetics Analysis (Mixed Model) analysing the inhibition of r3β-HSD4 by eight different parabens (A-G). Incubation conditions included a temperature of 37°C, with pregnenolone (0.2 mM), NAD^+ (0.2 mM), rat placental microsomes (10 μg), and varying concentrations of each paraben in 0.01 M PBS (pH 7.2). These plots provide a detailed view of the inhibition patterns and the impact of different paraben concentrations on enzyme activity.

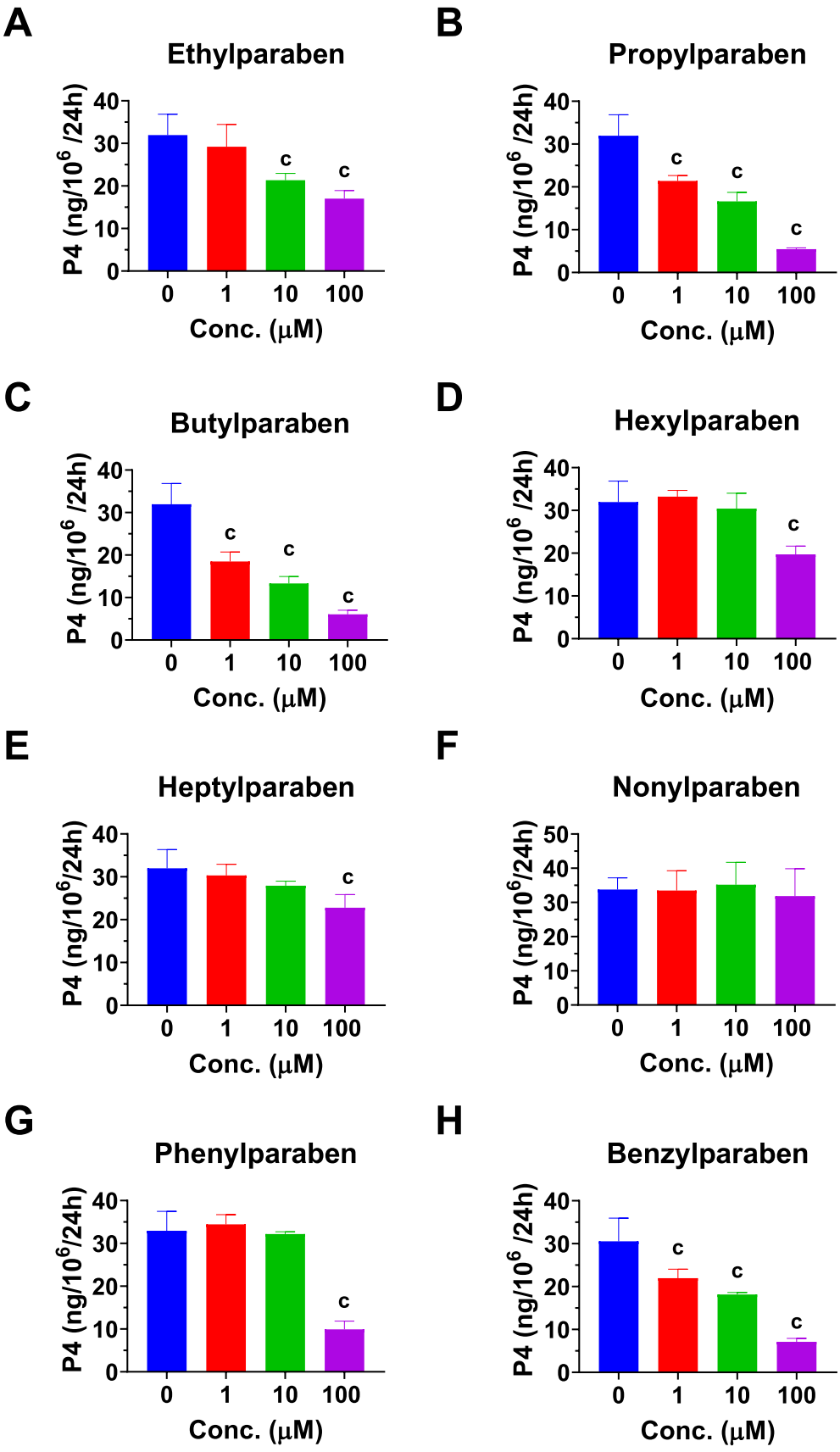

Fig. 5. Illustration of the impact of parabens on progesterone production by human JAr cells at concentrations of 1, 10, 50, and 100 μM. The graph compares progesterone output under basal conditions (A-H) with control samples, highlighting significant differences at ^{c} $P<0.001$ ($n = 4–16$, mean ± SEM) across all concentrations tested.

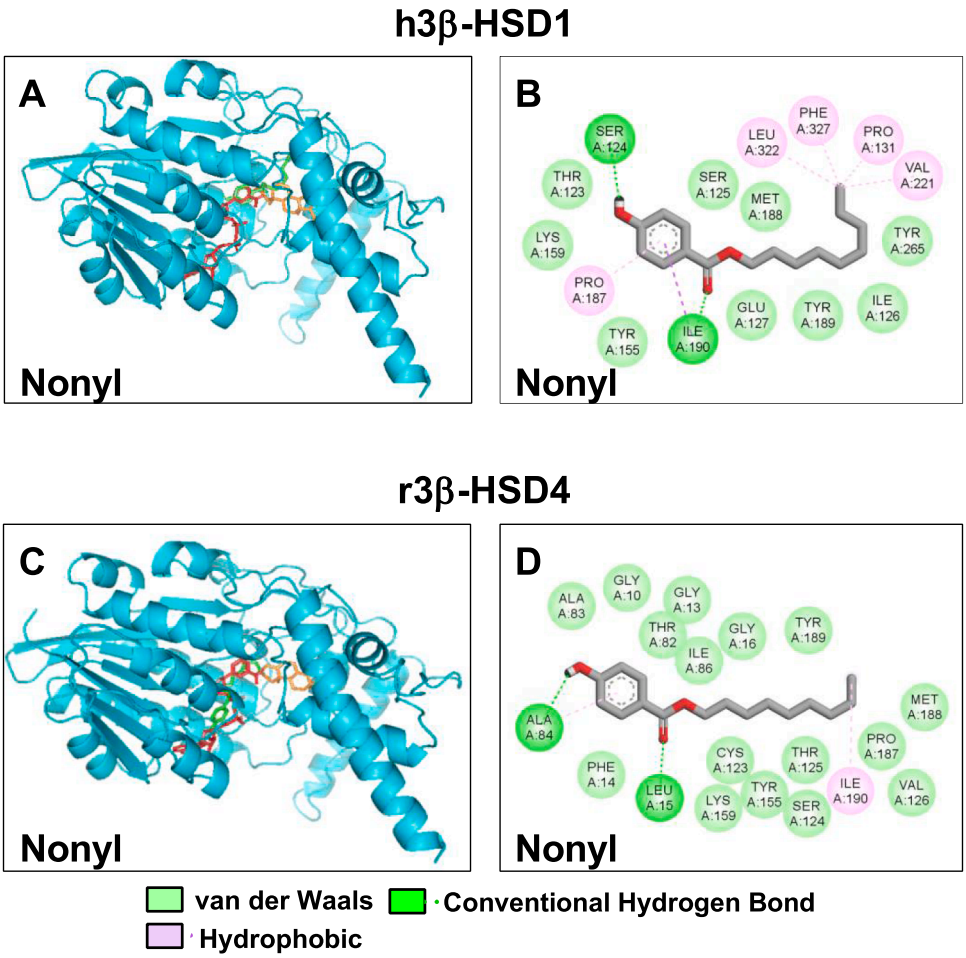

Fig. 6. Molecular docking studies of nonylparaben with human 3β-HSD1 (h3β-HSD1) and rat 3β-HSD4 (r3β-HSD4). This figure includes 3D and 2D structural representations of pregnenolone (P5) complexed with h3β-HSD1 (panels A and B) and r3β-HSD4 (panels C and D), providing insights into the binding interactions at the molecular level. Panels A and B: yellow colour, steroid; green colour, nonylparaben, and brown colour, NAD^+; Panels C and D: Green dash-line, hydrogen bonds; purple dash-line, hydrophobic interaction; light blue residue, van der Waals.

parabens inhibited h3β-HSD1 and r3β-HSD4 enzyme activity in a dose-dependent manner, with nonylparaben being the most potent inhibitor. The inhibition mode was identified as mixed/noncompetitive, and some parabens were found to suppress P4 secretion in human JAr cells. Docking simulations indicated that parabens interact with either NAD^+ binding sites or nearby region of both enzymes. A negative correlation between certain physicochemical properties and IC_{50} values emphasized the significance of carbon chain length and LogP in determining inhibitory efficacy.

These findings have several implications. Firstly, they provide valuable insights into the potential endocrine-disrupting effects of parabens. Parabens are widely used as preservatives in cosmetics, personal care products, foodstuff, and pharmaceuticals [1]. The ability of parabens to inhibit steroid dehydrogenases suggests that they may interfere with the normal function of the endocrine system, which could have implications for human health. Indeed, the inhibition of parabens on placental 3β-HSD activity could lead to reduced placental levels of P4, which plays critical role in pregnancy [26]. The inhibition of P4 biosynthesis could result in the abortion [27]. The inhibition of parabens on 3β-HSD isoforms may be due to their structural resemblance to steroid structure. Indeed, parabens have also demonstrated to inhibit other steroidogenic dehydrogenases, such as human 17β-HSD1 [10]. The inhibitory effects of parabens on different enzymes could have implications for various physiological processes and potentially contribute to the overall understanding of their endocrine-disrupting potential. Besides, parabens also bind to human estrogen receptor [28], which also causes endocrine disrupting effects. Further studies are needed to explore this possibility and determine the specific mechanisms and extent of inhibition.

Furthermore, the research underscored the necessity of evaluating the SAR of parabens. The findings revealed that the length of the carbon chain within parabens significantly influenced their inhibitory effectiveness. Specifically, parabens with longer carbon chains in their alcohol component exhibited greater inhibitory potency. This enhanced efficacy is likely attributable to the increased hydrophobic interactions facilitated by the extended carbon chain. It is well-established that a longer carbon chain correlates with higher lipophilicity, as indicated by a larger LogP value. Nevertheless, it is imperative to recognize that while parabens with longer chains may demonstrate increased inhibitory effects in a cell-free environment, their ability to permeate the cell membrane and impede P4 synthesis may be compromised. For instance, nonylparaben, despite being the most potent inhibitor in a cell-free system, failed to affect P4 synthesis in JAr cells, even when administered at a concentration of 100 μM.

In fact, the computer analysis carried out by ADMETlab 2.0 showed that as the carbon chain length in the alcohol moiety increased, there was a reduction in solubility (LogS) and permeability (in Caco-2 and MDCK cells, as shown in Table S1). This insight is invaluable for the rational design of preservatives that are both safer and more efficacious. Interestingly, carbon chain length of parabens also affects human 17β-HSD1 activity in a similar way [10].

The development of 3D-QSAR models for parabens with h3β-HSD1

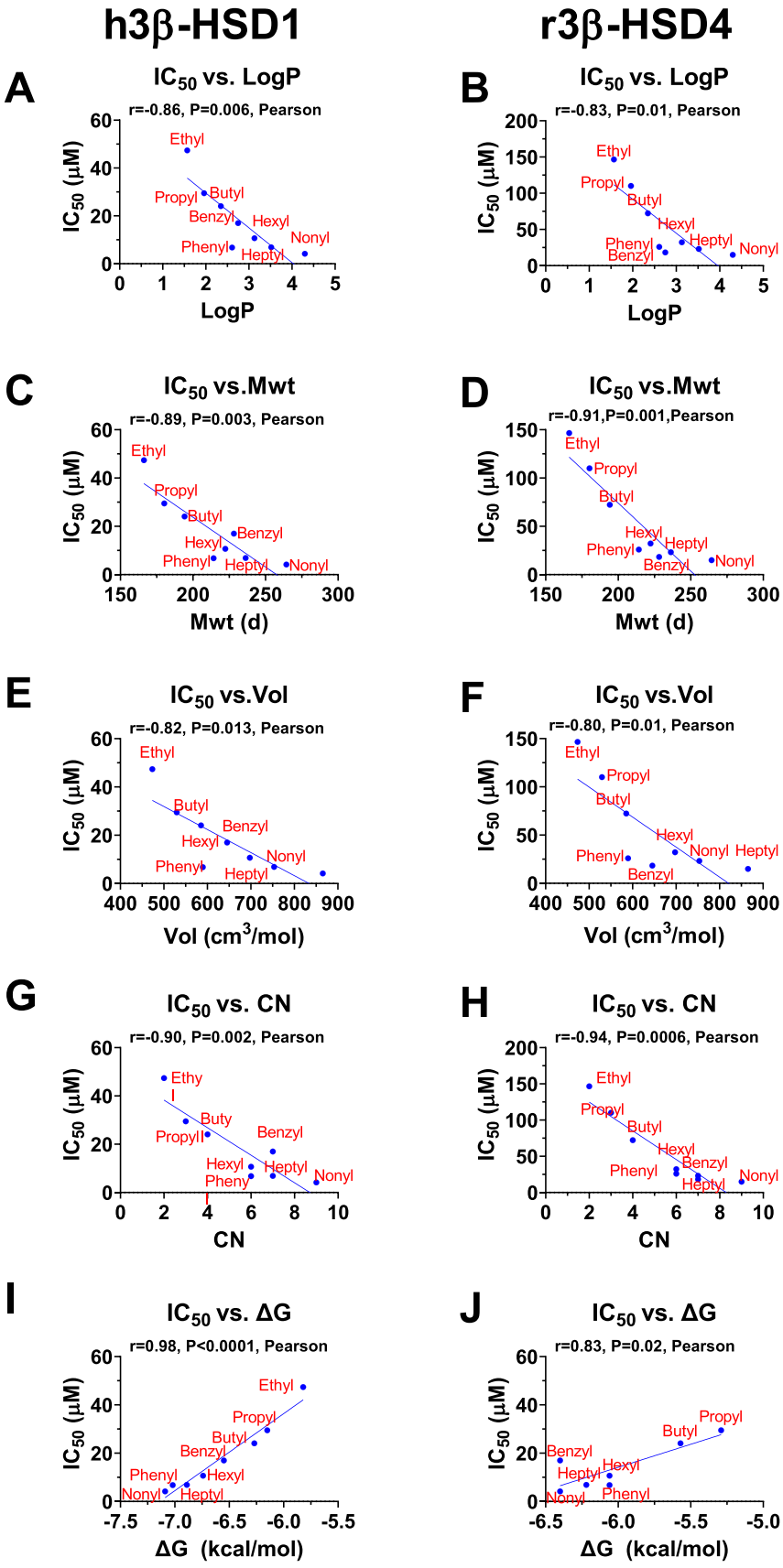

Fig. 7. IC_{50} value dependence on LogP, molecular weight (Mwt), volume, the number of carbon atoms, ΔG values in the alcohol moiety. This analysis is split between human 3β-HSD1 (h3β-HSD1, panels A, C, E, G, I) and rat 3β-HSD4 (r3β-HSD4, panels B, D, F, H, J), offering a comparative perspective on enzyme sensitivity.

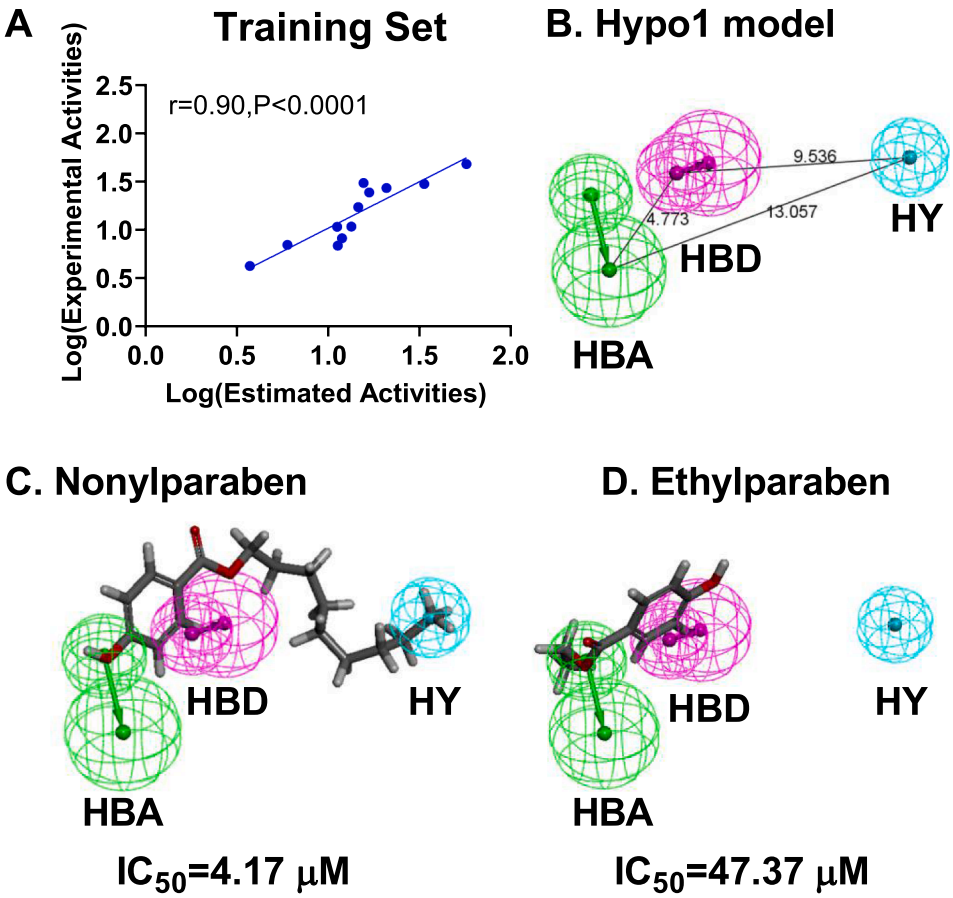

Fig. 8. 3D QSAR Hypo1 pharmacophore model of h3β-HSD1 inhibitors. Panel A evaluates the predictive efficacy of the model through a correlation plot between experimental and predicted activities of the training set compounds ($r = 0.90$, $P < 0.0001$). Panel B details the pharmacophore features of the Hypo1 model, including hydrogen bond acceptors (HBA, green), hydrogen bond donors (HBD, purple), and hydrophobic regions (HY, blue), with distances between features specified in angstroms. Panels C and D contrast the most active compound, nonylparaben (IC50 = 4.17 μM; fit value = 2.68), with the less potent ethylparaben (IC50 = 47.37 μM; fit value = 1.78), illustrating the model's utility in predicting compound efficacy.

activity is a significant step in understanding the structural requirements for potent inhibitors of this enzyme. The focus on three pivotal features—HBA (Hydrogen Bond Acceptor), HBD (Hydrogen Bond Donor), and HY (Hydrophobic regions)—along with the recognition of LogP (octanol-water partition coefficient) as a critical determinant of inhibition, provides a comprehensive framework for analysing and predicting the activity of potential inhibitors. The identification of HBA, HBD, and HY as critical features in the pharmacophore models suggests that these elements are essential for the interaction between parabens and h3β-HSD1. This information can guide the design of new compounds that optimize these interactions to enhance inhibitory potency. The observation that larger LogP values correlate with stronger inhibition indicates that lipophilicity plays a significant role in the efficacy of parabens as inhibitors. This could be due to better membrane penetration, enhanced binding to the enzyme, or improved stability in biological systems. However, it is also important to consider the potential for increased toxicity or reduced solubility at very high LogP values. The 3D-QSAR models can help in identifying structural modifications that could identify the inhibitory activity of parabens. Although 3D-QSAR analysis is a valuable tool for drug discovery. Our research is primarily focused on identifying the hazards associated with these compounds. This 3D-QSAR analysis has the significance in the context of hazard identification.

Furthermore, the docking simulations provide a mechanistic understanding of how parabens interact with the enzymes. We created h3β-HSD1 3D model, which was similar to the model created Thomas group [29,30]. This model shows the catalytic residues are Ser124, Tyr155, and Lys159. Most parabens bind to the NAD^+ binding site or approximate to the NAD^+ binding site suggests a mixed/noncompetitive inhibition mechanism. This is an important observation as it provides insights into the mode of action of parabens on 3β-HSD isoforms. The mixed/noncompetitive inhibition implies that parabens interact with both the enzyme and the substrate, potentially affecting the binding and catalytic activity of the enzyme. Further studies are needed to confirm and elucidate the detailed mechanism of this inhibition. Understanding the interaction between parabens and the NAD^+ binding site could help in the development of strategies to mitigate their inhibitory effects or design alternative compounds with reduced inhibitory potential. Additionally, this information could contribute to a better understanding of the potential endocrine-disrupting effects of parabens and their implications for human health.

Interestingly, the inhibitory effects of parabens on r3β-HSD4 have similar inhibition trend although we found that r3β-HSD4 is less sensitive to their inhibition than h3β-HSD1. This species-dependent difference has implications. Since r3β-HSD4 plays a role in steroidogenesis and other physiological processes, understanding the impact of paraben inhibition on these processes is crucial. This could involve studying the effects of parabens on hormone levels, reproductive health, and overall metabolic function in animal models for extrapolations of human potential health effects. Comparing the sensitivity of r3β-HSD4 across different species could provide insights into species-specific vulnerabilities and help in extrapolating findings to humans. This could involve comparative biochemical and toxicological studies. Studying the dosage and exposure levels of parabens that lead to significant inhibition of r3β-

HSD4 could help in assessing the safety thresholds for these compounds. This could involve dose-response studies to determine the minimal effective concentration and the potential for cumulative effects.

The fact that all parabens tested were able to inhibit both h3β-HSD1 at concentrations in the μM range is an important observation from the *in vitro* experiments. These data suggest that parabens have the potential to interact with and inhibit these enzymes under experimental conditions. In contrast, human exposure to parabens typically occurs at nM levels. This vast difference in concentration between the *in vitro* inhibitory concentrations and the *in vivo* exposure levels raises questions about the physiological relevance of the *in vitro* findings. At nM levels of exposure, the probability of parabens reaching sufficient concentrations to inhibit these enzymes *in vivo* seems low. Although the individual levels of parabens in the body are typically in the nM range, it is important to consider the potential for cumulative effects. Humans are exposed to multiple parabens simultaneously from various sources, such as personal care products and food. The combined effect of different parabens and their metabolites may potentially reach levels that could have a more significant impact on enzyme inhibition. However, more research is needed to understand whether such cumulative effects could occur and whether they would be sufficient to inhibit h3β-HSD1 *in vivo*. There may be certain populations that are more susceptible to the effects of parabens on these enzymes. For example, individuals with impaired metabolism or those with pre-existing conditions that affect the normal function of h3β-HSD1 may be more vulnerable. In these cases, even the relatively low levels of parabens in the body could potentially have a more pronounced effect on enzyme activity. Future studies should focus on identifying such susceptible populations and understanding the potential implications for their health.

In conclusion, the study contributes to our understanding of the potential endocrine-disrupting effects of parabens by inhibiting placental 3β-HSDs and provides important information for the development of safer alternatives. Further research is needed to investigate the long-term effects of parabens on human health and to explore potential strategies for minimizing their impact.

CRediT authorship contribution statement

Qian Zhang: Methodology. **Mingzhu Zhong:** Methodology, Formal analysis. **Jie Xiang:** Writing – original draft, Validation, Methodology, Formal analysis. **Weibing Zhang:** Formal analysis, Conceptualization. **Ren-shan Ge:** Writing – review & editing, Funding acquisition, Conceptualization. **Rongying Ou:** Writing – review & editing. **Qianjin Fei:** Supervision. **Huitao Li:** Software, Formal analysis. **Peipei Pan:** Methodology. **Yang Zhu:** Software.

Declaration of Competing Interest

The authors declare that they have no known competing financial interests or personal relationships that could have appeared to influence the work reported in this paper.

Acknowledgments

This work was supported by NSFC (82371610 to R.S.G and 82201856 to P.P.). We also thank Scientific Research Center of Wenzhou Medical University for consultation and instrument availability that supported this work.

Appendix A. Supporting information

Supplementary data associated with this article can be found in the online version at doi:10.1016/j.jsbmb.2024.106638.

Data Availability

No data was used for the research described in the article.

References

[1] A.R. Pereira, M. Simões, I.B. Gomes, Parabens as environmental contaminants of aquatic systems affecting water quality and microbial dynamics, Sci. Total Environ. 905 (2023) 167332.
[2] L. Stroppel, T. Schultz-Fademrecht, M. Cebulla, M. Blech, R.J. Marhöfer, P. M. Selzer, P. Garidel, Antimicrobial preservatives for protein and peptide formulations: an overview, Pharmaceutics 15 (2023).
[3] J.Y. Kim, Y. Park, S.H. Lee, E.J. Park, H.J. Lee, Comparative study on estrogen receptor alpha dimerization and transcriptional activity of parabens, Toxicol. Res 40 (2024) 153–161.
[4] J. Vitku, T. Skodova, A. Varausova, L. Gadus, L. Michnova, L. Horackova, L. Kolatorova, M. Simkova, J. Heracek, Endocrine disruptors and estrogens in human prostatic tissue, Physiol. Res 72 (2023) S411–S422.
[5] X. Niu, G. Chen, Y. Chen, N. Luo, M. Wang, X. Hu, Y. Gao, Y. Ji, T. An, Estrogenic effect mechanism and influencing factors for transformation product dimer formed in preservative parabens photolysis, Toxics 11 (2023).
[6] P.D. Darbre, Endocrine disrupting chemicals and breast cancer cells, Adv. Pharm. 92 (2021) 485–520.
[7] J. Kiwitt-Cárdenas, J.J. Arense-Gonzalo, E. Adoamnei, L. Sarabia-Cos, F. Vela-Soria, M.F. Fernández, J. Gosálvez, J. Mendiola, A.M. Torres-Cantero, Urinary concentrations of bisphenol A, parabens and benzophenone-type ultra violet light filters in relation to sperm DNA fragmentation in young men: A chemical mixtures approach, Sci. Total Environ. 912 (2024) 169314.
[8] T. Colnot, W. Dekant, H. Greim, Grouping of esters of 4-hydroxybenzoic acid for hazard assessment, Arch. Toxicol. 98 (2024) 571–575.
[9] S. Hassan, A. Thacharodi, A. Priya, R. Meenatchi, T.A. Hegde, T. R, H.T. Nguyen, A. Pugazhendhi, Endocrine disruptors: Unravelling the link between chemical exposure and Women's reproductive health, Environ. Res 241 (2024) 117385.
[10] R.T. Engeli, S.R. Rohrer, A. Vuorinen, S. Herdlinger, T. Kaserer, S. Leugger, D. Schuster, A. Odermatt, Interference of Paraben Compounds with Estrogen Metabolism by Inhibition of 17β-Hydroxysteroid Dehydrogenases, Int J. Mol. Sci. 18 (2017).
[11] Q. Zhu, P. Pan, X. Chen, Y. Wang, S. Zhang, J. Mo, X. Li, R.S. Ge, Human placental 3β-hydroxysteroid dehydrogenase/steroid Δ5,4-isomerase 1: Identity, regulation and environmental inhibitors, Toxicology 425 (2019) 152253.
[12] J. Simard, M.L. Ricketts, S. Gingras, P. Soucy, F.A. Feltus, M.H. Melner, Molecular biology of the 3beta-hydroxysteroid dehydrogenase/delta5-delta4 isomerase gene family, Endocr. Rev. 26 (2005) 525–582.
[13] T.E. White, R.A. Saltzman, P.A. Di Sant'Agnese, P.C. Keng, R.M. Sutherland, R. K. Miller, Human choriocarcinoma (JAr) cells grown as multicellular spheroids, Placenta 9 (1988) 583–598.
[14] R.A. Xu, B. Mao, S. Li, J. Liu, X. Li, H. Li, Y. Su, G. Hu, Q.Q. Lian, R.S. Ge, Structure-activity relationships of phthalates in inhibition of human placental 3β-hydroxysteroid dehydrogenase 1 and aromatase, Reprod. Toxicol. 61 (2016) 151–161.
[15] S. Wang, B. Zhang, Y. Zhai, Y. Tang, Y. Lou, Y. Zhu, Y. Wang, R.S. Ge, H. Li, Structure-activity relationship analysis of perfluoroalkyl carbonic acids on human and rat placental 3β-hydroxysteroid dehydrogenase activity, Toxicology 480 (2022) 153334.
[16] X. Zhao, M. Ji, X. Wen, D. Chen, F. Huang, X. Guan, J. Tian, J. Xie, J. Shao, J. Wang, L. Huang, H. Lin, L. Ye, H. Chen, Effects of Midazolam on the development of adult leydig cells from stem cells in vitro, Front Endocrinol. (Lausanne) 12 (2021) 765251.
[17] T. Ongtanasup, S. Wanmasae, S. Srisang, C. Manaspon, S. Net-Anong, K. Eawsakul, In silico investigation of ACE2 and the main protease of SARS-CoV-2 with phytochemicals from Myristica fragrans (Houtt.) for the discovery of a novel COVID-19 drug, Saudi J. Biol. Sci. 29 (2022) 103389.
[18] T. Ongtanasup, A. Mazumder, A. Dwivedi, K. Eawsakul, Homology Modeling, Molecular docking, molecular dynamic simulation, and drug-likeness of the modified alpha-mangostin against the β-tubulin protein of acanthamoeba keratitis, Molecules 27 (2022).
[19] C. Gong, S. Chen, Y. Tang, H. Chen, J. Xie, Y. Lv, Z. Shen, Y. Zhu, S. Wang, R.S. Ge, J. Zhao, Effects of organochlorine pesticides on human and rat 17β-hydroxysteroid dehydrogenase 1 activity: Structure-activity relationship and in silico docking analysis, J. Steroid Biochem Mol. Biol. 240 (2024) 106510.
[20] J.J. Irwin, B.K. Shoichet, ZINC–a free database of commercially available compounds for virtual screening, J. Chem. Inf. Model 45 (2005) 177–182.
[21] G. Xiong, Z. Wu, J. Yi, L. Fu, Z. Yang, C. Hsieh, M. Yin, X. Zeng, C. Wu, A. Lu, X. Chen, T. Hou, D. Cao, ADMETlab 2.0: an integrated online platform for accurate and comprehensive predictions of ADMET properties, Nucleic Acids Res 49 (2021) W5–W14.
[22] M. Su, L. Ye, Y. Tang, S. Wang, Z. Hu, H. Li, Y. Wang, X. Li, Y. Liu, R.S. Ge, Inhibition of resveratrol analogs on human and rat 3β-hydroxysteroid dehydrogenases: structure-activity relationship and docking analysis, J. Agric. Food Chem. 71 (2023) 7566–7574.
[23] S. Wang, H. Lu, Y. Zhai, Y. Tang, M. Su, H. Li, Y. Wang, Y. Liu, R.S. Ge, Inhibition of human and rat placental 3β-hydroxysteroid dehydrogenases by bisphenol A analogues depends on their hydrophobicity: In silico docking analysis, Chem. Biol. Inter. 403 (2024) 111251.

[24] T. Matsunaga, S. Endo, S. Maeda, S. Ishikura, K. Tajima, N. Tanaka, K. T. Nakamura, Y. Imamura, A. Hara, Characterization of human DHRS4: an inducible short-chain dehydrogenase/reductase enzyme with 3beta-hydroxysteroid dehydrogenase activity, Arch. Biochem Biophys. 477 (2008) 339–347.
[25] S. Ohno, N. Matsumoto, M. Watanabe, S. Nakajin, Flavonoid inhibition of overexpressed human 3beta-hydroxysteroid dehydrogenase type II, J. Steroid Biochem Mol. Biol. 88 (2004) 175–182.
[26] M. Hill, A. Pašková, R. Kančeva, M. Velíková, J. Kubátová, L. Kancheva, K. Adamcová, M. Mikešová, Z. Žižka, M. Koucký, H. Šarapatková, V. Kačer, P. Matucha, M. Meloun, A. Pařízek, Steroid profiling in pregnancy: a focus on the human fetus, J. Steroid Biochem Mol. Biol. 139 (2014) 201–222.
[27] N. Chabbert-Buffet, G. Meduri, P. Bouchard, I.M. Spitz, Selective progesterone receptor modulators and progesterone antagonists: mechanisms of action and clinical applications, Hum. Reprod. Update 11 (2005) 293–307.
[28] J.R. Byford, L.E. Shaw, M.G. Drew, G.S. Pope, M.J. Sauer, P.D. Darbre, Oestrogenic activity of parabens in MCF7 human breast cancer cells, J. Steroid Biochem Mol. Biol. 80 (2002) 49–60.
[29] J.L. Thomas, W.L. Duax, A. Addlagatta, L.A. Scaccia, K.A. Frizzell, S.B. Carloni, Serine 124 completes the Tyr, Lys and Ser triad responsible for the catalysis of human type 1 3beta-hydroxysteroid dehydrogenase, J. Mol. Endocrinol. 33 (2004) 253–261.
[30] J.L. Thomas, R. Huether, V.L. Mack, L.A. Scaccia, R.C. Stoner, W.L. Duax, Structure/function of human type 1 3beta-hydroxysteroid dehydrogenase: an intrasubunit disulfide bond in the Rossmann-fold domain and a Cys residue in the active site are critical for substrate and coenzyme utilization, J. Steroid Biochem Mol. Biol. 107 (2007) 80–87.